PSEUDO-DUCTILE CARBON/EPOXY HYBRID COMPOSITES

Gergely Czél[1,2], Meisam Jalalvand[3] and Michael Wisnom[4]

[1]MTA–BME Research Group for Composite Science and Technology
Budapest University of Technology and Economics, Műegyetem rkp. 3. H-1111 Budapest, Hungary
Email: czel@pt.bme.hu, web page: http://www.pt.bme.hu/kutato/index.php?l=a

[2]Advanced Composites Centre for Innovation and Science, University of Bristol
Queen's Building, BS8 1TR, Bristol, United Kingdom
Email: G.Czel@bristol.ac.uk, web page: http://www.bristol.ac.uk/composites/

[3]Advanced Composites Centre for Innovation and Science, University of Bristol
Queen's Building, BS8 1TR, Bristol, United Kingdom
Email: M.Jalalvand@bristol.ac.uk, web page: http://www.bristol.ac.uk/composites/

[4]Advanced Composites Centre for Innovation and Science, University of Bristol
Queen's Building, BS8 1TR, Bristol, United Kingdom
Email: M.Wisnom@bristol.ac.uk, web page: http://www.bristol.ac.uk/composites/

Keywords: Hybrid composites, Pseudo-ductility, Fragmentation

ABSTRACT

Three different unidirectional interlayer hybrid composite configurations comprising different grades of carbon fibre/epoxy prepregs were designed and tested. The design of the hybrid configurations was based on two simple criteria to assure sufficient strength of the higher strain material layer and to avoid unstable delamination at the first fracture of the lower strain material layer. One of the three tested configurations demonstrated a favourable pseudo-ductile failure character along with outstanding initial stiffness and up to 1% pseudo-ductile strain between the first fracture and the final failure. A recently developed representation of the predicted failure sequence in the form of damage mode maps was applied to the tested configurations to understand the observed failure modes better. Good correlation was confirmed between the predictions and the experimental results; therefore the validity and merit of this new design tool was highlighted.

1 INTRODUCTION

High performance polymer matrix carbon fibre composites are utilised traditionally for a very demanding set of applications including military and civil aerospace, spacecraft, motorsports and high specification sport equipment (e.g. bicycle frames, golf shafts, tennis racquets etc.) for their exceptional specific stiffness and strength, fatigue and corrosion resistance. However, a fundamental limitation of current carbon fibre reinforced composites is their inherent brittleness. Failure can be sudden and catastrophic, with little or no warning and usually poor residual load-bearing capacity if any. This unfavourable failure character of carbon composites representing a significant risk of unexpected catastrophic fractures is usually compensated for by very conservative design limits and hinders component producers from exploiting the excellent mechanical properties of these materials.

High performance ductile composites showing a safe failure character are therefore of significant interest and could extend the scope of applications towards new fields such as automotive or construction where sudden failure is not tolerated. This may be achieved by the development of new composite materials demonstrating a gradual failure with features similar to ductile metals' failure such as yielding and strain-hardening which can preserve the load carrying capacity and integrity of seriously damaged structures. Clear and detectable warning before final failure indicating the onset and accumulation of damage in the material is also a key safety feature to realise.

These aims are very ambitious given that the traditional constituent materials of high performance composites such as glass, carbon fibres and epoxy resins are all brittle. The High Performance Ductile Composites Technology (HiPerDuCT) programme aims at exploring various ductility concepts utilising approaches ranging from the development of new ductile fibres/matrices to modification of the architecture of the composite laminates based on commercially available materials to allow one or more of the previously identified ductility mechanisms to be exploited. The second group of approaches can lead to pseudo-ductile materials, despite the fact that the constituents are all brittle. Interlayer (or layer-by layer) hybridisation of unidirectional (UD) glass and thin-ply carbon fibre reinforced epoxy showed very good potential for pseudo-ductility in tensile loading [1]. The thin-ply hybrid composite specimens showed stable fragmentation and pull-out of the carbon layer due to the low amount of energy released by the thin plies after their fractures during the mode II inter-laminar fracture propagation (layer pull-out) phase.

The aim of the reported research is to extend the recently demonstrated thin-ply glass/carbon hybrid composites ductility concept towards higher performance material combinations utilising pairs of different (high strength HS/high modulus HM) grade carbon fibre/epoxy prepregs. The proposed HS carbon/epoxy-HM carbon/epoxy hybrid composite configurations are expected to show similar linear-plateau-linear style stress-strain graphs to those of the glass-carbon hybrids, but with higher initial modulus, which is required by industries such as aerospace which traditionally utilise high stiffness and lightweight carbon fibre composite materials to increase the efficiency of their products.

2 MATERIAL AND CONFIGURATION DESIGN

This section gives details of the applied materials and the design considerations to assure a stable pseudo-ductile failure of the hybrid laminates.

2.1 Materials

The materials considered for design, and used in the experimental part of the study were thin T1000 carbon/epoxy, M40 carbon/epoxy, M46 carbon/epoxy and XN80 carbon/epoxy prepregs manufactured by North Thin Ply Technology Ltd. The resin type in all the prepregs were North TPT's ThinPreg 120 EPHTg- 402 type 120°C cure, medium viscosity, toughened epoxy system. Properties of the applied fibres and composite prepregs can be found in Tables 1 and 2.

Carbon fibre type	Manufacturer	Elastic modulus	Strain to failure	Tensile strength	Density
		[GPa]	[%]	[GPa]	[g/cm^3]
Torayca T1000	**Toray**	294	2.2	6.37	1.80
Torayaca M40JB	**Toray**	377	1.2	4.40	1.75
Torayaca M46JB	**Toray**	436	0.9	4.02	1.84
Granoc XN80	**Nippon GFC**	780	0.5	3.43	2.17

Table 1: Fibre properties of the applied UD prepregs based on manufacturer's data

Prepreg material	Fibre mass per unit area	Cured ply thickness	Fibre volume fraction	Initial elastic modulus
	[g/m^2]	[µm]	[%]	[GPa]
T1000/epoxy	28	32.4	48	143
M40/epoxy	40	42.5	54	204
M46/epoxy	29	29.7	53	233
XN80/epoxy	50	46.7	49	387

Table 2: Material properties of the cured UD thin composite plies applied (All figures are based on/calculated from manufacturer's data.)

2.2 Design of hybrid laminates

Figure 1 shows the interlayer hybrid composite laminate design comprising a central HM carbon layer with low failure strain and two outer HS carbon layers with high failure strain. When the hybrid specimen is loaded in tension, the central low strain layer starts fracturing first, and the load is shed to the outer high strain layers. If the hybrid configuration is carefully designed for pseudo-ductility, the low strain layer should show multiple fragmentation and stable delamination from the high strain layers without any significant load drop until the final failure of the hybrid material.

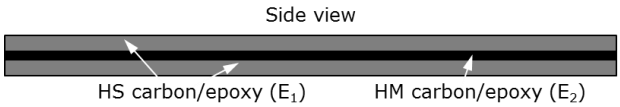

Figure 1: Interlayer hybrid composite laminate design

We identified and published the following design criteria earlier [1] to assure stable pseudo-ductile failure for UD glass/carbon interlayer hybrids. The same criteria are adapted here for the similar configuration with new sets of constituent prepregs:
(i) The outer, high strain layers need to be thick enough to take the full load after low strain material fracture and pull-out with a sufficient margin required to account for stress concentrations which are not considered in this approach.

$$\sigma_{1b} > \frac{\sigma_{2b}(2E_1t_1 + E_2t_2)}{2E_2t_1} \tag{1}$$

Where E_1 is the modulus of the high strain (HS carbon) layers, E_2 is the modulus of the low strain (HM carbon) layer, t_1 is the thickness of one high strain (HS carbon) layer (see Figure 2), t_2 is the thickness of the low strain (HM carbon) layer, σ_{1b} is the strength of the high strain (HS carbon) layers, σ_{2b} is the strength of the low strain (HM carbon) layer.

(ii) The energy release rate (G_{II}) at the expected failure strain of the low strain (HM carbon) layer must be lower than the mode II fracture toughness (G_{IIC}) of the interface to avoid mode II delamination of the central low strain layer after its first fracture. This criterion assures the condition for the multiple fractures (i.e. fragmentation) and stable pull-out of the low strain layer.

$$G_{IIC} > G_{II} = \frac{\varepsilon_{2b}^2 E_2 t_2 (2E_1t_1 + E_2t_2)}{8E_1t_1} \tag{2}$$

Where ε_{2b} is the failure strain of the low strain (HM carbon) layer.

Table 3 shows the configurations designed according to equations (1) and (2). It is worth noting that an advantageous high HM/HS carbon ratio with the currently available minimum ply thicknesses can be achieved only if a very high modulus central layer is applied, which starts failing at low strains therefore keeping the G_{II} low. The other thing to note is that all the predicted G_{II} values are lower than the typical G_{IIC}=1 N/mm for this type of epoxy matrix UD prepreg composites, therefore fragmentation and stable pull-out of the central HM carbon layer is expected.

Spec. Type	Fibre masses per unit area	Nominal thickness	Nominal HM/HS carbon volume ratio	Predicted G_{II} at HM carbon failure strain
	[g/m^2]	[mm]	[-]	[N/mm]
5T1000/2M40/5T1000	140/80/140	0.409	0.29	0.860
3T1000/3M46/3T1000	84/87/84	0.284	0.51	0.734
2T1000/2XN80/2T1000	56/100/56	0.223	0.74	0.666

Table 3: Interlayer hybrid configurations (Numbers in the specimen designation indicate the number of thin prepreg plies.)

3 EXPERIMENTAL

This section describes the specimen geometry, composite processing and sample fabrication as well as the test equipment and procedure applied.

3.1 Specimen geometry and manufacturing

Figure 2 shows the geometric parameters on the side and top view schematics of an interlayer hybrid composite tensile specimen.

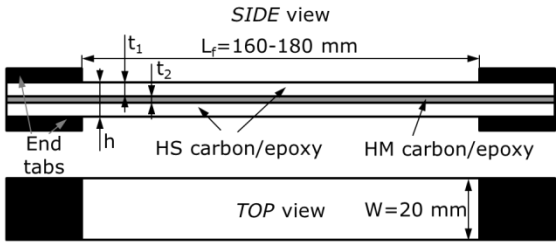

Figure 2: Schematic of the specimen geometry

The UD hybrid composite plates were manufactured by hand lay-up stacking the specified prepreg plies on top of each other keeping the same fibre direction and curing them in an autoclave according to the recommended cycle (2 hours at 120°C). Since all prepreg materials had the same matrix, there were no problems with bonding between the layers. Individual specimens were fabricated with a diamond cutting wheel, and 40 mm long, 2 mm thick cross-ply glass/epoxy end-tabs were bonded on them.

3.2 Test method

Testing of the parallel edge specimens was executed under uniaxial tensile loading and displacement control using a crosshead speed of 2 mm/min on a computer controlled Instron 8801 type 100 kN rated universal hydraulic test machine with wedge type hydraulic grips. Strains were measured using an Imetrum videogauge system, with a nominal gauge length of 130 mm.

3.3 Results and discussion

Figure 3. shows the stress-strain curves of the 5T1000/2M40/5T1000 type specimens. This series of specimens showed unfavourable catastrophic failure for three of the six specimens tested. The other three specimens showed a few large load drops before final failure but this behaviour was not acceptable for pseudo-ductility. The first load drop occurred at strains close to the HM carbon fibre failure strain.

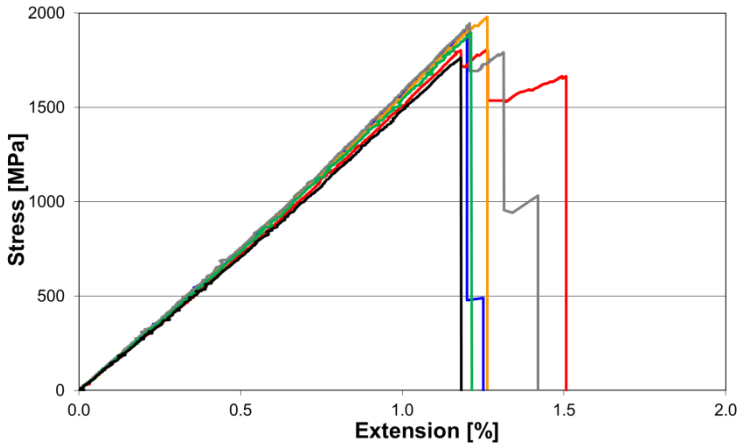

Figure 3: Test results of the 5T1000/2M40/5T1000 type specimens

Figure 4 shows the stress-strain response of 3T1000/3M46/3T1000 type specimens. This configuration demonstrated a gradual failure starting at strains slightly lower than the failure strain of the M46 fibres. Although the observed failure type was not catastrophic, the extent of the load drops was too high to render this response pseudo-ductile.

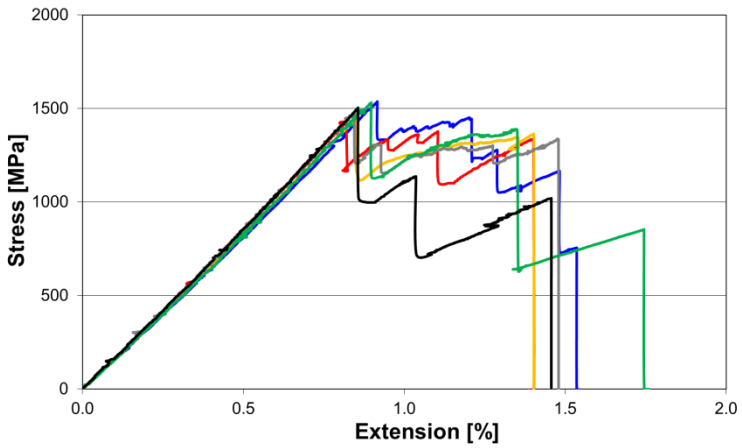

Figure 4: Test results of the 3T1000/3M46/3T1000 type specimens

Figure 5 shows the stress-strain graphs of 2T1000/2XN80/2T1000 type specimens. This configuration demonstrated a favourable pseudo-ductile failure process comprising a linear, a plateau and a second rising part in the stress-strain graphs. During the initial linear phase the material did not encounter significant damage and the modulus was simply determined by the constituent HM and HS carbon fibre composite layers. The first fracture in the HM carbon layer occurred around 0.4% strain, which is significantly lower than the 0.5% fibre failure strain quoted in the datasheet of the fibres. It was followed by fragmentation (i.e. multiple fractures) of the HM carbon layer until saturation of the cracks. Finally the HS carbon layers started to carry even more load and allowed for a second, quasi-linear rising part in the stress-strain curve.

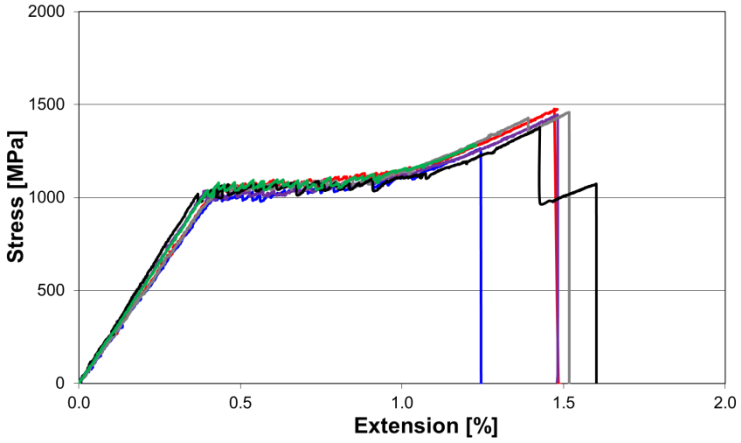

Figure 5: Test results of the 2T1000/2XN80/2T1000 type specimens

Table 4 summarises the results of the tensile tests for the three configurations. The pseudo-yield strain and stress were taken from the first knee point on the stress-strain graph of the 2T1000/2XN80/2T1000 configuration. It is worth highlighting that the initial modulus of this successful configuration was increased by up to 80% compared to that of the high strain material (T1000/epoxy) of the hybrid plate. On the other hand, the pseudo-yield stress of this configuration, which can be interpreted as a design stress is reduced by a factor of almost two, compared to the highest strength (lowest ductility) 5T1000/2M40/5T1000 configuration. The observed strong trade-off between stiffness and strength is based on the mechanical properties of the available carbon fibre grades, but hybridisation was able to add a key extra feature to the stiffest grade: a 1% strain margin between the onset of damage and final failure which can be exploited for structural health monitoring and warning before failure.

Spec. type		**Nominal HM/HS carbon volume ratio**	**Initial modulus**	**Modulus increase to T1000**	**Pseudo-yield/ first drop strain**	**Pseudo-yield/ first drop stress**	**Approx. final failure strain**	**Pseudo-ductile strain**
		[%]	**[GPa]**	**[%]**	**[%]**	**[MPa]**	**[%]**	**[%]**
5T1000/2M40/ 5T1000	**Av[a]**	0.294	145.9	2.5	1.21	1882	1.30	-
	CoV[b]	-	3.0	-	3.4	4.4	9.7	-
3T1000/3M46/ 3T1000	**Av**	0.507	162.6	13.7	**0.86**	1489	1.51	-
	CoV	-	2.3	-	4.1	2.8	8.7	-
2T1000/2XN80/ 2T1000	**Av**	0.741	256.5	79.4	**0.41**	1036	1.47	0.96
	CoV	-	5.2	-	6.0	1.3	9.2	-

[a]Average
[b]Coefficient of variation

Table 4: Summary of test results (Modulus and stress values were calculated with nominal thicknesses)

In order to find the possible reasons for the unfavourable failure character of the first two specimen configurations, careful observation of the failed specimens was carried out. The failure of 5T1000/2M40/5T1000 type specimens was explosive, therefore it was hard to establish the failure sequence. Observation of the remaining pieces revealed, that a significant part of the specimen was

delaminated, but splitting was dominant as well, together with the presence of local fibre fractures. As three of the specimens showed load drops, it is likely, that the first failure type right after HM carbon fracture was delamination in those specimens. The specimens showing catastrophic failure probably encountered delamination and HS carbon layer fracture simultaneously at the first HM carbon layer fracture.

Extensive delamination was observed for 3T1000/3M46/3T1000 type failed specimens: the layers of the hybrid materials were separated over most of the volume of the specimens and there was no obvious sign of coincident through thickness cracks in the originally adjacent layers. This suggests that the final failure of the specimens was not triggered by an overall catastrophic fracture of all the layers at the same position due to stress concentrations from the fragmenting HM carbon layer. The load drops on the stress-strain curves indicate, that the specimens probably delaminated at the first HM carbon layer fracture.

The extent of the first unstable delamination and the corresponding load drop under displacement control is governed by the energy release rate at the strain of carbon fracture and the mode II fracture toughness of the specimen configuration, therefore the more catastrophic behaviour of the 5T1000/2M40/5T1000 type is understandable since its energy release rate is higher, as shown in Table 3.

The energy release rate of the 3T1000/3M46/3T1000 specimen type was lower, therefore the extent of the delamination at first HM carbon layer fracture was expected to be smaller, so the HS carbon layer could survive it, allowing for a more gradual failure process. Later, other HM carbon layer fractures (and limited delamination) could take place resulting in further load drops in parallel with other failure modes e.g. splitting along the fibres due to localised fibre fractures.

According to the above mentioned observations and attempts to estimate the failure mode sequence of the specimen types, the following possible reasons for premature failure were identified:

(i) The actual G_{IIC} of the applied interlayer hybrid materials was significantly lower than the assumed typical value (1 N/mm). (ii) The recorded final failure strains (i.e. at failure of the T1000/epoxy layers) were significantly lower than that quoted for the T1000 fibres. This may have been the consequence of prepreg manufacturing defects (minor fibre waviness was observed during lay-up of the plies) and stress concentrations around the low strain (HM carbon) layer fractures and the end-tabs.

In order to understand the failure mechanisms better, a novel representation of the damage modes of interlayer hybrid composites developed recently by Jalalvand et al [2, 3] was applied to the tested configurations of this study. Each damage mode map in Figure 6 was generated assuming a typical G_{IIC}=1 N/mm fracture toughness and first HM carbon layer fracture at the failure strain of the corresponding constituent fibres (based on manufacturer's data in Table 1). The high strain material failure was predicted using a statistical strength distribution based on the fibre strain and typical Weibull parameters for high strength carbon fibres. Stress concentrations around the fractured low strain layer were taken into account as explained in [2]. The maps show the expected damage modes and the achievable pseudo-ductile strains for the selected configurations marked with circles. The coloured regions of the map indicate pseudo-ductile failure and the white region shows premature failure due to various reasons. All the expected damage modes for the four regions are described in Figure 6b. The pseudo-ductile strain is defined between a point at the initial slope line at failure stress and the final failure strain as shown on Figure 7.

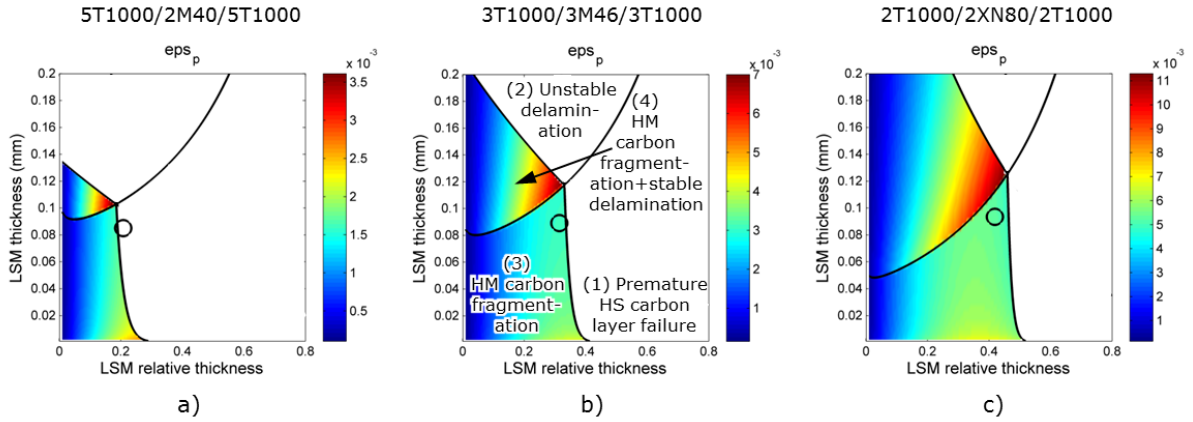

Figure 6: Damage mode maps of the tested configurations with G_{IIC}=1 N/mm: a) 5T1000/2M40/5T1000, b) 3T1000/3M46/3T1000, c) 2T1000/2XN80/2T1000, (eps_p is the predicted pseudo-ductile strain, LSM is the Low Strain Material- HM carbon in this study and the relative thickness is calculated as HM carbon thickness/full specimen thickness)

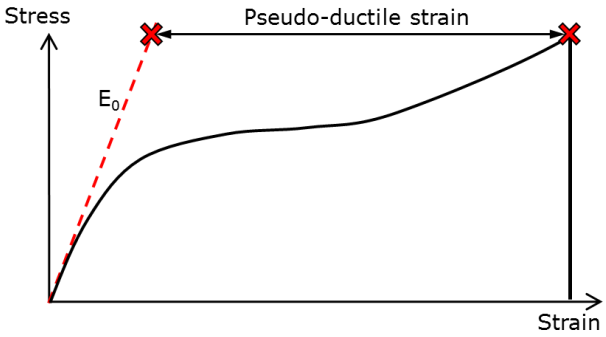

Figure 7: Definition of pseudo-ductile strain

Figure 6a shows that the 5T1000/2M40/5T1000 configuration should fail catastrophically because of the weak HS carbon layer (due to its too low thickness). Please note that the analytical equations applied to draw the damage mode maps, take the stress concentrations around fractures in the HM carbon layer into account, which was not incorporated in the simple design equations used earlier in this study therefore the premature failure in the experiments was unexpected. The stress concentration is especially pronounced in regions (1) and (3) of the maps (see fig 6b) under the positive slope inclined line which indicates the limit for delamination. No delamination is predicted for this configuration although the more gradual failure with multiple load drops of three specimen and the observations of the failed specimens suggested the presence of this damage type.

The marker for the 3T1000/3M46/3T1000 configuration in Figure 6b is very close to the boundary for catastrophic failure, therefore transitional behaviour might be expected. This configuration showed significant drops on the stress-strain curves each of which probably corresponded to limited but unstable delamination of the layers triggered by the first HM carbon layer fracture. Since the map does not show any delamination for this configuration, it is likely, that the G_{IIC} assumed for the maps is too high for the material system applied.

Figure 6c confirms the pseudo-ductile response of the 2T1000/2XN80/2T1000 configuration through fragmentation of the HM carbon layer in the hybrid. This successful configuration generated up to 1% pseudo-ductile strain and exhibited a very high initial stiffness due to the ultra-high modulus carbon central layer. The damage mode map however, only shows 0.5% pseudo-ductile strain for this configuration with the current input parameters which is only half of the experimental result.

A second set of damage mode maps shown in Figure 8 were generated to incorporate some of the

experimental observations in the model such as the realistic failure strains of the XN80 and M46 carbon layers (using the bold values in Table 3). The mode II fracture toughness of the layer interfaces was also modified to one half of the originally assumed value based on test results of other interlayer hybrid configurations with the same resin system, where a change from unstable to stable failure was observed around G_{II}=0.5 N/mm. The failure strains of M40 and T1000 layers were not changed.

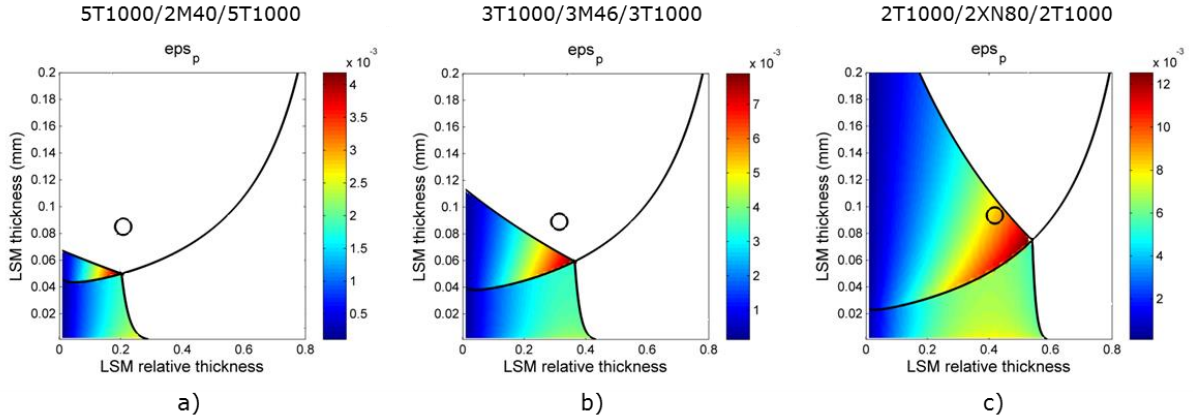

Figure 8: Damage mode maps of the tested configurations with G_{IIC}=0.5 N/mm and experimentally determined failure strains for M46/epoxy and XN80/epoxy layers: a) 5T1000/2M40/5T1000, b) 3T1000/3M46/3T1000, c) 2T1000/2XN80/2T1000, (eps_p is the predicted pseudo-ductile strain, LSM is the Low Strain Material- HM carbon in this study and the relative thickness is calculated as HM carbon thickness/full specimen thickness)

The updated map in Figure 8a shows unstable delamination instead of overall catastrophic failure (i.e. fracture of all layers) for the 5T1000/2M40/5T1000 configuration, due to the lower G_{IIC} used. This agrees with the observations made on the failed specimens. Delamination typically releases the direct stress concentrations on the high strain layer therefore saving it from instantaneous failure after the first crack in the low strain layer. The catastrophic failures observed experimentally for three of the six specimens indicate that this configuration was also prone to HS carbon layer failure due to stress concentrations around the HM layer fractures and the end tabs.

Unstable delamination is now shown for 3T1000/3M46/3T1000 type specimens as well (see Figure 8b), which could result in significant load drops and a gradual decrease of stress as observed on the experimental stress-strain curves. The released energy was significantly lower for this configuration and therefore the high strain layers were able to survive the first delamination, however they probably suffered significant damage as indicated by the gradual decrease of the stress on the stress-strain curves instead of an expected rising part after delamination if the high strain layer would have remained intact.

The damage mode map in Figure 8c for 2T1000/2XN80/2T1000 type specimens changed significantly by using more realistic input parameters. The lower failure strain (0.41%) for the low strain material extended the allowable relative thickness of HM carbon layer significantly which could be useful for designing even higher performance configurations. The shown damage mode was changed from fragmentation to fragmentation+stable delamination, which can provide higher pseudo-ductile strain. The predicted amount of pseudo-ductile strain agrees with the experiments for this set of input parameters.

Although the damage mode maps were applied here for damage analysis only, they proved the strong potential for supporting the design of pseudo-ductile interlayer hybrid composites provided accurate input parameters are available.

4 CONCLUSIONS

The following conclusions were drawn from the study of high modulus (HM)-high strength (HS) carbon/epoxy interlayer hybrid composites:

- The thin-ply hybrid composite ductility concept was successfully extended to high performance HM carbon-HS carbon/epoxy hybrid material combinations.
- One of the developed unidirectional HM carbon-HS carbon/epoxy hybrid composite materials exhibited outstanding initial modulus up to 257 GPa and up to 1% pseudo-ductile strain before final failure in tension.
- The wide margin between the first fracture in the high modulus carbon layer and final failure of the hybrid laminate can act as a clear and detectable warning sign which can make the operation of a component made of the new pseudo-ductile material safer.
- The damage mode maps were helpful in explaining the experimentally observed failure types, which highlights the merit of this new tool in the design of unidirectional interlayer hybrid composites.

ACKNOWLEDGEMENTS

This work was funded under the UK Engineering and Physical Sciences Research Council (EPSRC) Programme Grant EP/I02946X/1 on High Performance Ductile Composite Technology in collaboration with Imperial College, London. Gergely Czél acknowledges the Hungarian Academy of Sciences for funding through the Post-Doctoral Researcher Programme fellowship scheme. The authors thank North Thin Ply Technology for the supplied materials.

REFERENCES

[1] G. Czél, M.R. Wisnom, Demonstration of pseudo-ductility in high performance glass-epoxy composites by hybridisation with thin-ply carbon prepreg. *Composites Part A: Applied Science and Manufacturing*, **52**, 2013, pp. 23-30 (doi:10.1016/j.compositesa.2013.04.006)

[2] M. Jalalvand, G. Czél, M.R. Wisnom, Damage analysis of pseudo-ductile thin-ply UD hybrid composites - A new analytical method, *Composites Part A: Applied Science and Manufacturing*, **69**, 2015, pp. 83-93 (doi: 10.1016/j.compositesa.2014.11.006)

[3] M. Jalalvand, G. Czél, M.R. Wisnom, Parametric study of failure mechanisms and optimal configurations of pseudo-ductile thin-ply UD hybrid composites, *Composites: Part A: Applied Science and Manufacturing*, **74**, 2015, pp. 123-131 (doi:10.1016/j.compositesa.2015.04.001)